Applied Physics
Express

LETTER • OPEN ACCESS

Si-doped AlN using pulsed metalorganic chemical vapor deposition and doping

To cite this article: Tariq Jamil *et al* 2025 *Appl. Phys. Express* **18** 025501

OPEN ACCESS

Applied Physics Express 18, 025501 (2025) LETTER

https://doi.org/10.35848/1882-0786/adadc2

Si-doped AlN using pulsed metalorganic chemical vapor deposition and doping

Tariq Jamil[1*], Abdullah Al Mamun Mazumder[1], Mafruda Rahman[1], Muhammad Ali[1], Jingyu Lin[2], Hongxing Jiang[2], Grigory Simin[1], and Asif Khan[1]

[1]Department of Electrical Engineering, University of South Carolina, Columbia, SC 29208, United States of America
[2]Department of Electrical & Computer Engineering, Texas Tech University, TX 79409, United States of America

*E-mail: tjamil@email.sc.edu

Received December 21, 2024; revised January 18, 2025; accepted January 23, 2025; published online February 6, 2025

In this paper we describe a pulsed metalorganic chemical vapor deposition (MOCVD) Si-doping approach for AlN epilayers over bulk AlN. The Al-rich growth/doping conditions in the pulsed MOCVD process resulted in n-AlN layers with transmission line model currents that were an order higher than for structures on layers that were grown/doped at identical temperatures using the conventional MOCVD process. Our work demonstrated that like the other reported approaches such as UV exposure during growth, the pulsed MOCVD process is also very effective in reducing point defects by the defect quasi-Fermi level-chemical potential control. © 2025 The Author(s). Published on behalf of The Japan Society of Applied Physics by IOP Publishing Ltd

AlN is an excellent choice for high-temperature, and high-power electronic devices. With an extremely high breakdown field (~14–16 MV cm^{-1}), and thermal conductivity (~300 W m-K^{-1}), its Baliga figure of Merit (BFOM) is higher than other wide bandgap or extreme bandgap (EBG) semiconductors such as SiC, GaN, Ga_2O_3, and $Al_xGa_{x-1}N$ ($x \geqslant 60$).[1,2] However, till recently the progress towards AlN for power and optical devices was limited due to the difficulty in *n*- or *p*-type doping which was partly due to the high ionization energy of the Si-donor (~280 MeV) and the Mg-acceptor (~630 MeV).[3,4] In addition, the high growth temperatures required for the metalorganic chemical vapor deposition (MOCVD) process also led to the formation of self-compensating defects there by limiting the free electron concentration in Si-doped AlN.[5] In their early work, Taniyasu et al. reported the room-temperature carrier concentration and the mobility for their MOCVD grown Si-doped AlN layers to be around $(0.8–1.7) \times 10^{15}$ cm^{-3}, and (426–125) cm^2 V^{-1} s^{-1}.[6–8] To date there are no reports of *p*-type doping in AlN using MOCVD.

Recently Ahmed et al. reported very high *n*-type and *p*-type conductivity in AlN using Si- and Be- with a low temperature (~800 °C–900 °C) metal modulated molecular beam epitaxy (MME) process.[9–13] They attributed their high conductivity values to the low growth temperature which leads to a significant reduction in the formation of self-compensating defects. Moreover, the metal-rich growth conditions enabled reduction in the Al-Vacancy-Si complexes which behave analogously to Al-Vacancy-O complexes resulting in the self-compensation of the donors. The metal rich growth can also improve doping by the control of the chemical potential/quasi-Fermi energy. Mudiyanselage et al., and Quinones et al. reported on lateral and quasi-vertical conduction Schottky barriers on Si-doped AlN layers grown on bulk AlN use conventional MOCVD process with growth temperatures around 1100 °C–1250 °C.[14–18] For their conventional MOCVD process the Al- and N- precursors (Trimethylaluminum and Ammonia), and the Si-dopant were simultaneously introduced in the growth chamber. Quinones et al. reported the room temperature carrier concentration and Hall mobility for their growths to be 1.5×10^{15} cm^{-3} and 160 cm^2 V^{-1} s^{-1}, respectively. They employed a Hg-lamp irradiation for Fermi level control to mitigate the self-compensation thereby increasing the Si-doping.[19–21] Bulk AlN substrates are now readily available from several vendors with the defect levels ~10^3 cm^{-2}.[22,23] For both Mudiyanselage and Da B et al.[14,18] the surface ohmic contacts to the doped AlN layers were nonlinear at low voltages. They measured and reported their contact and sheet resistivity values at room and elevated temperatures using the linear *I*–*V* region.

In this paper we report a new migration enhanced Pulsed MOCVD (PMOCVD) process with a site selection silicon doping scheme for *n*-AlN epilayers on bulk AlN. The structural, optical and electrical characteristics of these were compared to layers that were grown using the conventional MOCVD growth/doping approach reported in Refs. 14, 18.

In Fig. 1 we show the precursor flows as a function of time for the conventional and the PMOCVD processes used for our study. In the past, the PMOCVD process has been shown to yield much smoother surface morphology in III-N epilayer growth due to reduced gas phase adduct formation.[24–26] Furthermore, the increased mobility of the Al-precursors on the growth surface (in absence of NH_3) leads to high quality epitaxy even at temperatures which are 150 °C–200 °C lower than those used for conventional MOCVD.[27] As seen from Fig. 1, we introduced the Si-dopant in the epi-growth under metal rich conditions i.e. with the Al-pulse. In our study, the conventional and PMOCVD growths were carried out under identical conditions at ~1100 °C and 40 torr. This was the surface temperature measured by a pyrometer. Prior to the growth, the c-oriented bulk AlN substrates were cleaned in organic solvents (acetone, IPA), followed by an acid clean (NH_4OH, HCl, HF). They were also annealed under NH_3 at 1150 °C. Trimethylaluminum (TMA), ammonia (NH_3), and silane (SiH_4) were used as aluminum, nitrogen, and silicon precursors, respectively. A 200 nm thick undoped AlN layer was first grown at 1150 °C using conventional MOCVD followed by 200 nm thick Si-doped AlN layers using both the conventional and the PMOCVD processes of Fig. 1.

In Fig. 2(a) we include the surface atomic force microscope (AFM) scans for the conventional and the PMOCVD *n*-AlN layers. Despite the high Si-doping, both the layers were very smooth with their RMS surface roughness values,

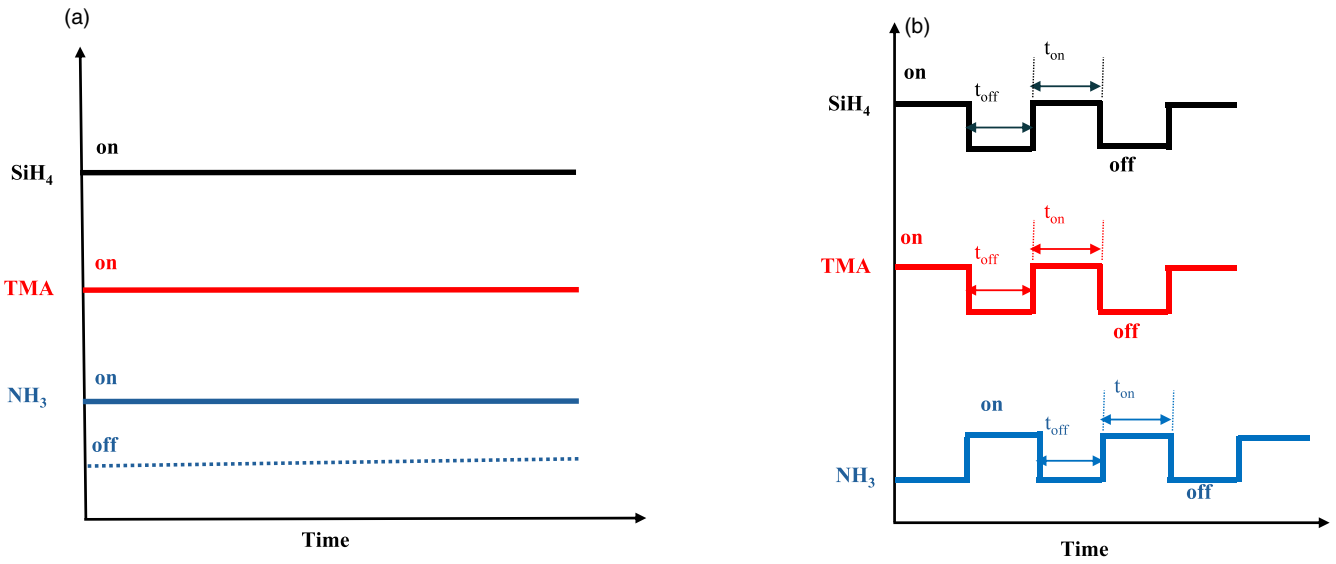

Fig. 1. (a) Precursor time-flow sequence for the conventional growth, (b) Pulsed MOCVD growth. Si-dopant are introduced with Al-pulse for metal rich condition.

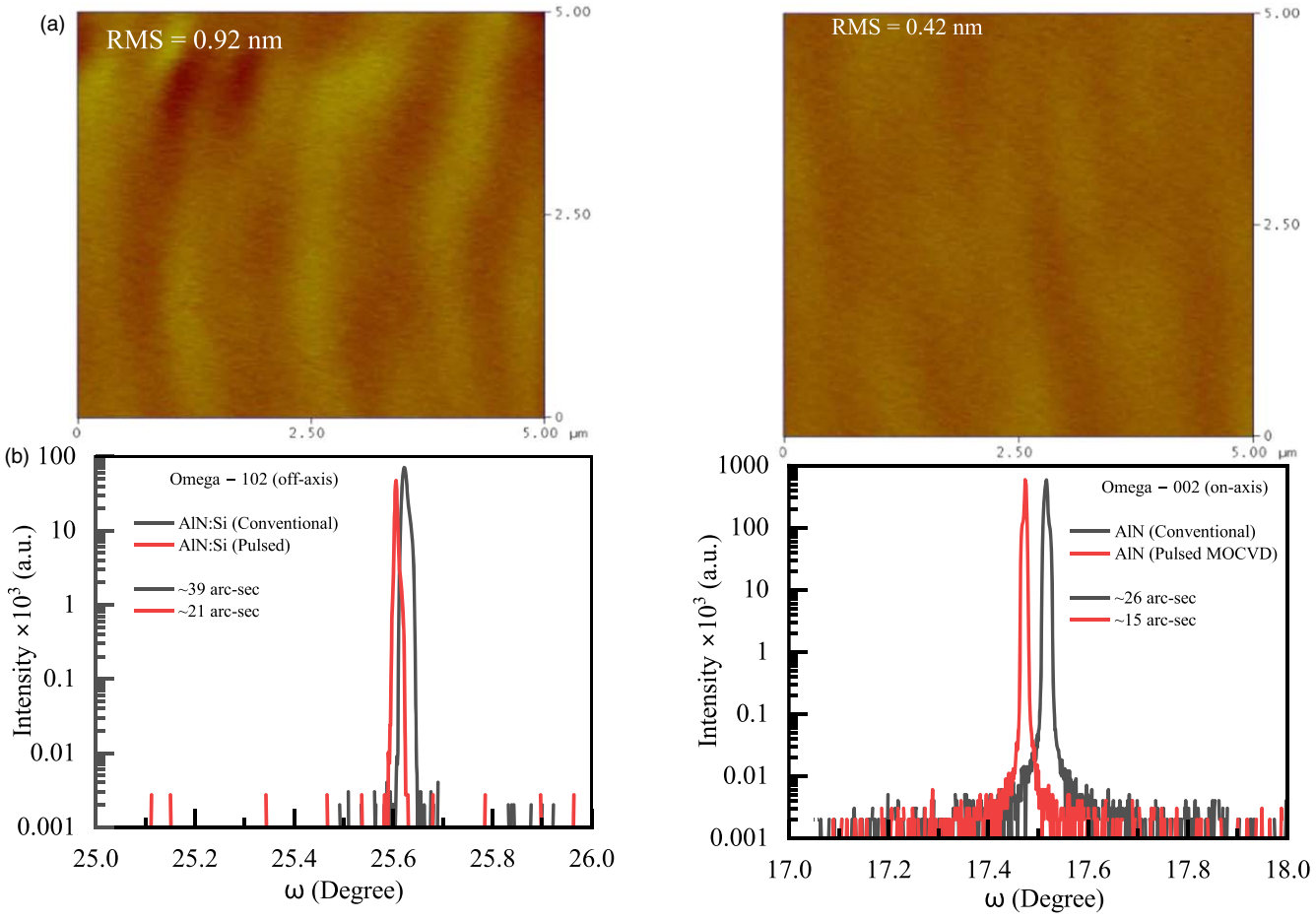

Fig. 2. (a) AFM surface scans of n-AlN layers of the study (right) conventional growth having roughness ∼0.92 nm and (left) the PMOCVD growth having roughness ∼0.42 nm on 5 × 5 μm^2 area. (b) HRXRD off-axis (1012) and on-axis (0002) scans of the conventional and the PMOCVD *n*-AlN layers of the study. The off-axis and on-axis FWHM is slightly lower in the case of PMOCVD n-AlN layer.

respectively 0.92 and 0.42 nm. In Fig. 2(b) High resolution X-ray diffraction measurements show the off-axis (1012) and on-axis (0002) for conventional and PMOCVD *n*-AlN layers. The off-axis (1012) linewidths were ∼39 and ∼21 arcsec, and the on-axis (0002) linewidths were ∼26 and ∼15 arcsec, for the conventional and the PMOCVD *n*-AlN layers, respectively. It is worth noting that the PMOCVD *n*-AlN layers off-axis and on-axis are very close to that measured for the starting substrate. Using Reciprocal Space Lattice Mapping we confirmed our conventional and the PMOCVD *n*-AlN epilayer structures to be pseudomorphic. We therefore estimate the dislocation density in our *n*-AlN layers to be around 10^3 cm^{-2}

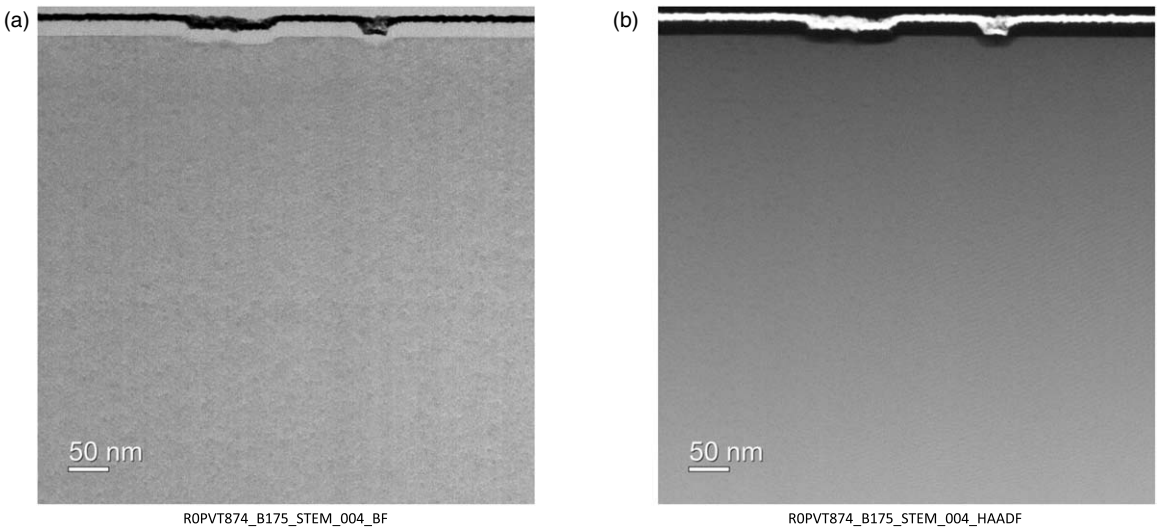

Fig. 3. High-resolution cross-section TEM for the PMOCVD *n*-AlN (a) Bright Field (BF) and (b) high-angle annular dark-field (HAADF) images. No dislocation generation was observed at the buffer AlN/AlN substrate or the Si-doped AlN/AlN buffer interface.

which is the same as for the bulk AlN substrate. This is also supported by the cross-section TEM data of Fig. 3.

We also compared the room-temperature photoluminescence (PL) of the layers of our study. For these measurements an Excimer laser ($\lambda = 193$ nm) pump was used. These PL spectra for Si-doped conventional MOCVD, PMOCVD and undoped conventional and PMOCVD samples are included in Fig. 4. As seen, all the samples show AlN band-edge emission at 5.93 eV. The highest intensity observed was for the PMOCVD AlN layers, probably due to better quality as compared to the conventional AlN. In addition, for the Si-doped layers an additional peak was also observed at 3.2 eV. This peak has also been observed in previous reports of AlN photoluminescence and was attributed to Al-vacancy formation resulting from the Silicon doping.[28–30] This seems to be the case for our study as well, because the 3.2 eV peak is absent in the PL data for our undoped AlN epi-structures (see Fig. 4). Since both the conventional and the P-MOCVD samples were grown at the same temperature and show the 3.2 eV emission peak, their conductivity difference cannot be from the Al-vacancy/Si complexes. It may be due to the reduced number of point defects from the pulsed doping approach (see Ref. 21). Low-temperature PL studies are currently underway to clarify this and will be reported separately. By measuring the room-temperature PL for the starting AlN substrate, we verified that the additional peak in our PL data at 2.55 eV is from the starting bulk AlN substrate.

We then fabricated transmission line model (TLM) test structures with contact spacing from 2 to 20 μm on the conventional MOCVD and on the PMOCVD Si-doped layers of the study. For the ohmic contact metals we used Zr (150)/Al (1000)/Mo (400)/Au (300) Å. The contacts were annealed at 950 °C for 30 s. Note this is the same contact formation scheme we had used in our previously reported EBG MOSHEMT structures with $Al_{0.65}Ga_{0.35}N$ channel and $Al_{0.85}Ga_{0.15}N$ barrier layers.[31,32] In Fig. 5, we plot the current–voltage (I–V) curves for the 4 and the 8 μm spacings TLM electrodes for the Si-doped, conventional and the PMOCVD growths (see inset to Fig. 5). As seen at low currents the TLM contacts are nonlinear which makes the estimation of true contact resistance more difficult. This is

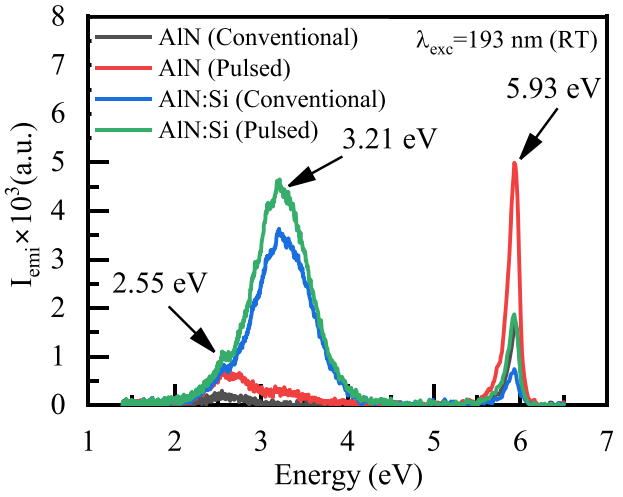

Fig. 4. Room temperature PL spectra for conventional and PMOCVD grown AlN films with and without Si-doping. The additional peak at 2.55 eV is from the AlN substrate.

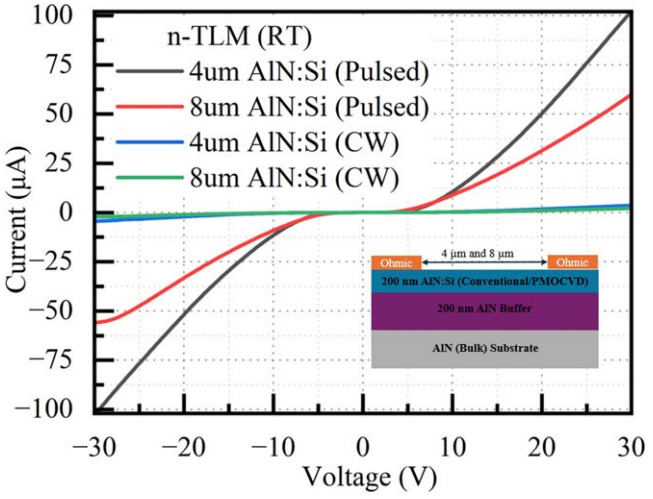

Fig. 5. Current–voltage characteristics of the 4 and 8 μm spacing TLM electrodes for the AlN:Si conventional and the PMOCVD layers. The inset shows the n-TLM scheme.

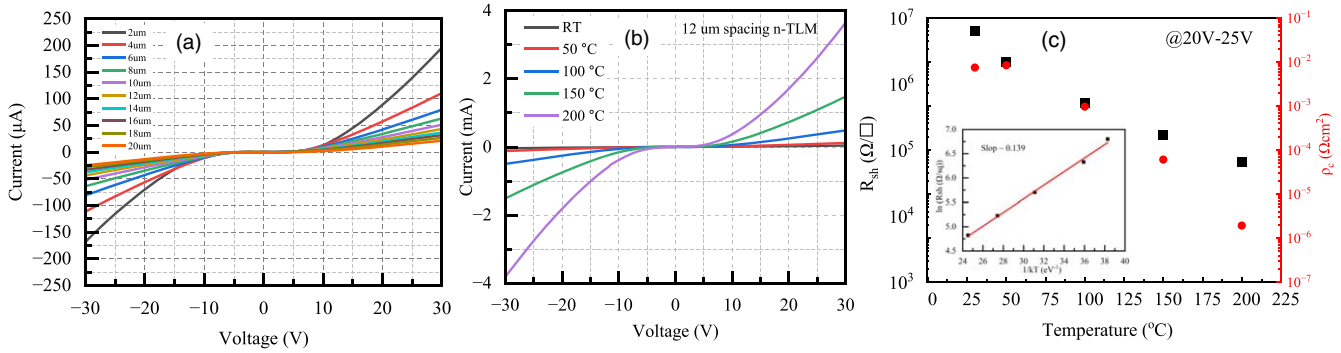

Fig. 6. (a) Room temperature TLM measurements for Si-doped PMOCVD AlN epilayers. (b) Temperature dependent *I*–*V* curves for the 12 μm spacing TLM electrodes for the sample of Fig. 6(a). (c) Sheet and contact resistivity as a function of temperature for the PMOCVD Si-doped n-AlN layers over bulk AlN substrates. Used the linear region for calculation from 20 to 25 V. The inset shows the extracted donor ionization energy which is ∼139 MeV.

like the observations of Mudiyanselage and Da B et al. From Fig. 5 data we see the peak current for the PMOCVD sample at a bias of 25 V, to be more than an order higher than the sample with conventional silicon doping. Since the growth temperatures for the two samples were the same, we conclude this increased current (doping) to be from the Metal-rich conditions employed for the silicon doping during the PMOCVD growth process. It should also be pointed out that these currents for the PMOCVD doped samples are also about an order higher than those reported by Mudiyanselage and Da B et al.[14,18)]

In Fig. 6(a) we have included the *I*–*V* characteristics of TLM structures for the PMOCVD Si-doped *n*-AlN sample. Using the slope of TLM *I*–*V* curves in the linear region (@25 V bias), the room-temperature sheet and contact resistivity values for our PMOCVD *n*-AlN samples were estimated to be 6.3 MΩ/□ and $7.4 \times 10^{-3}\,\Omega\,\mathrm{cm}^2$, respectively. These are lower than the values of the previous reports of Refs. 14–18 where an identical procedure was used to estimate the sheet and contact resistivity values. In Fig. 6(b) we show the 12 μm spacing TLM *I*–*V* data for the sample of Fig. 6(a) as a function of temperature from RT to 200 °C. From this temperature dependent data, we extracted the sheet resistance and the contact resistivity as a function of temperature. These data are plotted in Fig. 6(c). As seen, both the sheet and contact resistivity values decreased by several orders for a temperature rise from room to 200 °C. Quasi-linear logarithmic $R_{sh}(T)$ dependence suggests that the $R_{sh}(T)$ dependence is exponential and hence the main mechanism behind R_{sh} reduction is donor ionization. We then used the Arrhenius plot $\ln(R_{sh})$ versus $1/(kT)$ to extract the approximate value of donor ionization energy. When ignoring the relatively weak temperature dependence of carrier mobility, the extracted donor ionization energy was found to be $E_D \approx 139$ MeV [see the inset of Fig. 6(c)]. We have also estimated the Arrhenius slope correction due to mobility–temperature dependence. Assuming that mobility decreases roughly twice as the temperature increases from RT to 200 C (typical for wide bandgap alloys), the corrected donor ionization energy was estimated to be $E_D \sim 161$ MeV. Note that the obtained values of $E_D = 139$–161 MeV are significantly lower than 280 MeV reported in.[3,4)] This may be attributed to a different mechanism of Si incorporation in our PMOCVD growth process.

In conclusion, we have reported the use of pulsed MOCVD for Si-doped n-type AlN growth over bulk AlN. The site selection doping enabled Metal-rich conditions which led to doping and forward current density an order higher than other reports. Our work thus establishes the pulsed doping approach as an effective way to control point defects and defect quasi-Fermi level in *n*-type Si-doping of AlN layers over bulk AlN substrates.

Acknowledgments This material is based upon work supported by the Air Force Office of Scientific Research under award number FA9550-24-1-0269 (Dr. Ken Gorretta). Any opinions, findings, and conclusions or recommendations expressed in this material are those of the author(s) and do not necessarily reflect the views of the United States Air Force**.** It was also supported by USC Research Institute for Extreme Electronics' Grant No. 80005646.

ORCID iDs Tariq Jamil https://orcid.org/0000-0002-7321-4654 Jingyu Lin https://orcid.org/0000-0003-1705-2635

1) J. Y. Tsao, S. Chowdhury, M. A. Hollis, D. Jena, N. M. Johnson, K. A. Jones, and J. A. Simmons, Adv. Electron. Mater. **4**, 1600501 (2018).
2) A. V. Inyushkin, A. N. Taldenkov, D. A. Chernodubov, E. N. Mokhov, S. S. Nagalyuk, V. G. Ralchenko, and A. A. Khomich, J. Appl. Phys. **127**, 205109 (2020).
3) T. Kumabe, A. Yoshikawa, S. Kawasaki, M. Kushimoto, Y. Honda, M. Arai, and H. Amano, IEEE Trans. Electron Devices **71**, 3396 (2024).
4) R. Collazo, S. Mita, J. Xie, A. Rice, J. Tweedie, R. Dalmau, and Z. Sitar, Phys. Status Solidi c **8**, 2031 (2011).
5) J. Wang, F. Xu, L. Zhang, J. Lang, X. Fang, Z. Zhang, and B. Shen, J. Semicond. **45**, 021501 (2024).
6) Y. Taniyasu, M. Kasu, and N. Kobayashi, Appl. Phys. Lett. **81**, 1255 (2002).
7) Y. Taniyasu, M. Kasu, and T. Makimoto, Appl. Phys. Lett. **85**, 4672 (2004).
8) Y. Taniyasu, M. Kasu, and T. Makimoto, Nature **441**, 325 (2010).
9) W. A. Doolittle, C. M. Matthews, H. Ahmad, K. Motoki, S. Lee, A. Ghosh, and P. D. Yoder, Appl. Phys. Lett. **123**, 070501 (2023).
10) H. Ahmad, Z. Engel, C. M. Matthews, and W. A. Doolittle, J. Appl. Phys. **130**, 195702 (2021).
11) H. Ahmad, Z. Engel, C. M. Matthews, S. Lee, and W. A. Doolittle, J. Appl. Phys. **131**, 175701 (2022).
12) H. Ahmad, J. Lindemuth, Z. Engel, C. M. Matthews, T. M. McCrone, and W. A. Doolittle, Adv. Mater. **33**, 2104497 (2021).
13) H. Ahmad, K. Motoki, E. A. Clinton, C. M. Matthews, Z. Engel, and W. A. Doolittle, ACS Appl. Mater. Interfaces **12**, 37693 (2020).
14) D. H. Mudiyanselage, D. Wang, B. Da, Z. He, and H. Fu, Appl. Phys. Express **17**, 074001 (2024).
15) C. E. Quiñones, D. Khachariya, P. Bagheri, P. Reddy, S. Mita, R. Kirste, and Z. Sitar, Appl. Phys. Lett. **123**, 172103 (2023).
16) D. H. Mudiyanselage, D. Wang, B. Da, Z. He, and H. Fu, Appl. Phys. Express **17**, 014005 (2024).
17) C. Quiñones, D. Khachariya, P. Reddy, S. Mita, J. Almeter, P. Bagheri, and Z. Sitar, Appl. Phys. Express **17**, 101002 (2024).
18) B. Da, D. H. Mudiaynselage, D. Wang, Z. He, and H. Fu, Appl. Phys. Express **17**, 104002 (2024).

19) P. Reddy, S. Washiyama, F. Kaess, R. Kirste, S. Mita, R. Collazo, and Z. Sitar, J. Appl. Phys. **122**, 245702 (2017).
20) P. Reddy, M. P. Hoffmann, F. Kaess, Z. Bryan, I. Bryan, M. Bobea, and Z. Sitar, J. Appl. Phys. **120**, 185704 (2016).
21) P. Bagheri, C. Quiñones-Garcia, D. Khachariya, S. Rathkanthiwar, P. Reddy, R. Kirste, and Z. Sitar, J. Appl. Phys. **132**, 185703 (2022).
22) H. Helava, T. J. Chemekova, O. Avdeev, E. Mokhov, S. Nagalyuk, Y. Makarov, and M. Ramm, Phys. Status Solidi c **7**, 2115 (2010).
23) R. T. Bondokov, S. P. Branagan, N. Ishigami, J. Grandusky, T. Nagatomi, K. Tatsuta, and J. J. Chen, ECS Trans. **104**, 37 (2021).
24) M. A. Khan, R. A. Skogman, J. M. Van Hove, D. T. Olson, and J. N. Kuznia, Appl. Phys. Lett. **60**, 1366 (1992).
25) S. Y. Bae, K. Lekhal, H. J. Lee, J. W. Min, D. S. Lee, Y. Honda, and H. Amano, Phys. Status Solidi (b) **254**, 1600722 (2017).
26) K. M. Pürlü, M. N. Kocak, G. Yolcu, I. Perkitel, İ. Altuntaş, and I. Demir, Mater. Sci. Semicond. Process. **142**, 106464 (2022).
27) M. A. Khan, J. N. Kuznia, R. A. Skogman, D. T. Olson, M. Mac Millan, and W. J. Choyke, Appl. Phys. Lett. **61**, 2539 (1992).
28) N. Nepal, M. L. Nakarmi, J. Y. Lin, and H. X. Jiang, Appl. Phys. Lett. **89**, 092107 (2006).
29) K. B. Nam, M. L. Nakarmi, J. Y. Lin, and H. X. Jiang, Appl. Phys. Lett. **86**, 222108 (2005).
30) J. S. Harris, J. N. Baker, B. E. Gaddy, I. Bryan, Z. Bryan, K. J. Mirrielees, and D. L. Irving, Appl. Phys. Lett. **112**, 152101 (2018).
31) A. Mamun, K. Hussain, R. Floyd, M. D. Alam, M. V. S. Chandrashekhar, G. Simin, and A. Khan, Appl. Phys. Express **16**, 061001 (2023).
32) K. Hussain, A. Mamun, R. Floyd, M. D. Alam, M. E. Liao, K. Huynh, and A. Khan, Appl. Phys. Express **16**, 014005 (2023).